

# Influence of pair coherence on charge tunneling through a quantum dot connected to a superconducting lead

T. Domański, A. Donabidowicz, and K. I. Wysokiński

*Institute of Physics, M. Curie Skłodowska University, 20-031 Lublin, Poland*

(Received 18 December 2006; revised manuscript received 5 July 2007; published 19 September 2007)

We analyze the charge transport through a single level quantum dot coupled to a normal and superconducting lead where the electron pairs exist either as the coherent (for temperatures below  $T_c$ ) or incoherent objects (in a region  $T_c < T < T^*$ ). Practically, this situation can be encountered using the high  $T_c$  superconducting materials where precursor effects have been observed upon approaching  $T_c$  from above. Without restricting to any particular microscopic mechanism, we investigate the qualitative properties of nonequilibrium charge current caused by the electron pair coherence.

DOI: [10.1103/PhysRevB.76.104514](https://doi.org/10.1103/PhysRevB.76.104514)

PACS number(s): 74.45.+c, 74.20.Fg, 73.23.-b, 73.63.Kv

## I. INTRODUCTION

It is a well established experimental fact that phase transition from the normal to superconducting state of the underdoped high  $T_c$  copper oxides is accompanied by the appearance of a pseudogap.<sup>1</sup> Upon decreasing the temperature below  $T^*$  (larger than  $T_c$ ) the single particle states become gradually depleted over a certain energy region  $|\omega| < \Delta_{pg}$  around the Fermi level. This phenomenon is often interpreted theoretically as a precursor of the true superconducting gap usually present at temperatures  $T < T_c$ . On a microscopic level, the pseudogap can be assigned to the appearance of the electron pairs. Above  $T_c$ , their long-range coherence is missing because of the strong quantum fluctuations either driven by the reduced dimensionality, due to a close neighborhood to the Mott insulating state, or because of competition with some other types of ordering. The incoherent electron pairs have been unambiguously detected experimentally above  $T_c$  in measurements of the large Nernst coefficient<sup>2</sup> and in observation of the Berezinski-Kosterlitz-Thouless phase fluctuations.<sup>3</sup> There is, however, a great amount of controversy regarding the temperature extent where the incoherent pairs eventually exist. According to available experimental data, their presence has been confirmed at least for a dozen Kelvin above  $T_c$ , but such region might spread over a much wider regime, perhaps up to  $T^*$  where the pseudogap finally closes.

Various tunneling techniques have been used for a long time for probing the single particle spectra of the correlated systems. The recent technological progress of spectroscopic methods such as the scanning tunneling microscopy (STM),<sup>4</sup> the angle resolved photoemission spectroscopy (ARPES),<sup>5</sup> the Andreev-type techniques,<sup>6</sup> and the Fourier transformed scanning tunneling spectroscopy<sup>7</sup> allow for precise measurements of the energy, momentum, and spatially dependent density of states. They are hence useful for studying the pseudogap.

In the present work, we propose considering a spectroscopic method sensitive the coherence of electron pairs. For this purpose, we explore a junction consisting of a normal conductor coupled via the quantum dot to a superconducting electrode. We claim that in such setup, one could distinguish between the true gap and the pseudogap of the single particle

excitation spectrum. Pair coherence shows up there by the unique temperature dependence of the differential conductance (see Fig. 9 in Sec. V).

Our analysis here is not limited to any particular microscopic model describing the formation of electron pairs and onset of their coherence. We investigate on rather general grounds the proximity effect, which gives rise to a particle-hole mixing in the quantum dot spectrum at small energies  $|\omega| \leq \Delta$ , and analyze its influence on the nonequilibrium charge transport. We clear up few salient features typical for normal-quantum dot-superconductor N-QD-S junctions. In particular, for a limit of the strong on-dot repulsion, we report that the Kondo resonance enhances the Andreev conductance below the Kondo temperature  $T_K$  (assumed here to be smaller than  $T_c$ ). This aspect of our work clears up some earlier studies of the correlated quantum dot coupled between the normal and superconducting electrodes.

In Sec. II, we briefly introduce the problem explaining how we treat the coherent and incoherent electron pairs. Next, we discuss a spectrum of the quantum dot neglecting the correlations (Sec. III) and considering the limit of very strong on-dot interaction  $U = \infty$  (Sec. IV). The main part of our study is in Sec. V, where we determine the tunneling conductance as a function of bias  $V$  applied across N-QD-S junction for temperatures below and above  $T_c$ . In Sec. VI, we check an influence of the anisotropic  $d$ -wave energy gap and finally close the paper with summary and outlook for some related problems.

## II. FORMULATION OF THE PROBLEM

For a description of the quantum dot (QD) coupled to one normal ( $N$ ) and one superconducting ( $S$ ) leads, we consider the single impurity Anderson model

$$\hat{H} = \hat{H}_N + \hat{H}_S + \sum_{\sigma} \epsilon_d \hat{d}_{\sigma}^{\dagger} \hat{d}_{\sigma} + U \hat{n}_{d\uparrow} \hat{n}_{d\downarrow} + \sum_{\mathbf{k}, \sigma} \sum_{\beta \in \{N, S\}} [V_{\mathbf{k}\beta} \hat{d}_{\sigma}^{\dagger} \hat{c}_{\mathbf{k}\beta\sigma} + \text{H.c.}]. \quad (1)$$

Operators  $d_{\sigma}$  ( $d_{\sigma}^{\dagger}$ ) annihilate (create) electrons on the QD with a single particle energy  $\epsilon_d$ . Coulomb potential  $U > 0$  describes the repulsion between electrons of opposite spins

$\sigma = \uparrow, \downarrow$ . Hybridization  $V_{\mathbf{k}\beta}^*$  describes the transfer of electrons from the QD to the normal ( $\beta=N$ ) or superconducting ( $\beta=S$ ) leads.

We assume that the normal electrode is described by the Hamiltonian of noninteracting fermions,  $\hat{H}_N = \sum_{\mathbf{k},\sigma} (\varepsilon_{\mathbf{k}N} - \mu_N) \hat{c}_{\mathbf{k}\sigma N}^\dagger \hat{c}_{\mathbf{k}\sigma N}$ . To describe the superconducting lead, we use a general expression

$$\hat{H}_S = \sum_{\mathbf{k},\sigma} (\varepsilon_{\mathbf{k}S} - \mu_S) \hat{c}_{\mathbf{k}\sigma S}^\dagger \hat{c}_{\mathbf{k}\sigma S} + \hat{V}_{\text{pairing}}, \quad (2)$$

where the two-body term  $\hat{V}_{\text{pairing}}$  induces either coherent (below  $T_c$ ) or incoherent (above  $T_c$ ) electron pairs.

Without specifying  $\hat{V}_{\text{pairing}}$  nor restricting to any particular microscopic mechanism of superconductivity, we proceed along the lines of BCS-like treatment. For the superconducting state (below  $T_c$ ), we use the retarded Green's function in the Nambu representation given by the standard expression

$$G_S^r(\mathbf{k}, \omega) = \begin{pmatrix} \frac{u_{\mathbf{k}}^2}{\omega - E_{\mathbf{k}}} + \frac{v_{\mathbf{k}}^2}{\omega + E_{\mathbf{k}}} & \frac{u_{\mathbf{k}}v_{\mathbf{k}}}{\omega + E_{\mathbf{k}}} - \frac{u_{\mathbf{k}}v_{\mathbf{k}}}{\omega - E_{\mathbf{k}}} \\ \frac{u_{\mathbf{k}}v_{\mathbf{k}}}{\omega + E_{\mathbf{k}}} - \frac{u_{\mathbf{k}}v_{\mathbf{k}}}{\omega - E_{\mathbf{k}}} & \frac{v_{\mathbf{k}}^2}{\omega - E_{\mathbf{k}}} + \frac{u_{\mathbf{k}}^2}{\omega + E_{\mathbf{k}}} \end{pmatrix}, \quad (3)$$

where the quasiparticle dispersion is  $E_{\mathbf{k}} = \sqrt{\xi_{\mathbf{k}S}^2 + \Delta_{\mathbf{k}}^2}$  and  $\xi_{\mathbf{k}\beta} = \varepsilon_{\mathbf{k}\beta} - \mu_{\beta}$  measures the energy from the chemical potential  $\mu_{\beta}$ . As usual,  $\Delta_{\mathbf{k}}$  denotes a gap of the single particle excitations for  $S$  electrons, and the BCS coherence factors are  $u_{\mathbf{k}}^2 = \frac{1}{2} \left(1 + \frac{\xi_{\mathbf{k}S}}{E_{\mathbf{k}}}\right) = 1 - v_{\mathbf{k}}^2$ .

Since the excitation gap is known to develop well above the transition temperature, we follow the arguments of Chin *et al.*<sup>8</sup> and impose the following phenomenological ansatz for the effective gap:

$$\Delta_{\mathbf{k}}^2 = \Delta_{\mathbf{k},sc}^2 + \Delta_{\mathbf{k},pg}^2. \quad (4)$$

The first part  $\Delta_{\mathbf{k},sc}$  is related to the superconducting order parameter  $\langle \hat{c}_{-\mathbf{k}\downarrow S} \hat{c}_{\mathbf{k}\uparrow S} \rangle$ , while  $\Delta_{\mathbf{k},pg}$  refers to the pseudogap. For some quantitative study, we use temperature dependence in a form

$$\Delta_{\mathbf{k},sc}(T) = \begin{cases} \Delta_{\mathbf{k}}(0) \sqrt{1 - \left(\frac{T}{T_c}\right)^2} & \text{for } T \leq T_c \\ 0 & \text{for } T > T_c. \end{cases} \quad (5)$$

The pseudogap contribution  $\Delta_{\mathbf{k},pg}$  to the effective gap [Eq. (4)] originates from the preformed electron pairs, and above  $T_c$ , their long-range coherence is absent (hence, a name of the incoherent pairs). Such pairs ultimately dissociate at temperature  $T^*$ , so in analogy to Eq. (5), we propose

$$\Delta_{\mathbf{k}}(T) = \Delta_{\mathbf{k}}(0) \sqrt{1 - \left(\frac{T}{T^*}\right)^2}. \quad (6)$$

Above  $T_c$ , the off-diagonal long-range order is missing; therefore, the retarded Green's function [Eq. (3)] must reduce to a diagonal structure for an entire temperature region  $T_c < T < T^*$ . To satisfy this physical constraint, we set  $u_{\mathbf{k}}v_{\mathbf{k}} = \Delta_{\mathbf{k},sc}/2E_{\mathbf{k}}$ . Thus, above  $T_c$ , the pseudogap enters the Green's function only by the diagonal terms:<sup>8</sup>

$$G_S^r(\mathbf{k}, \omega) = \begin{pmatrix} \frac{u_{\mathbf{k}}^2}{\omega - E_{\mathbf{k}} + i\gamma_{\mathbf{k}}} + \frac{v_{\mathbf{k}}^2}{\omega + E_{\mathbf{k}} + i\gamma_{\mathbf{k}}} & 0 \\ 0 & \frac{v_{\mathbf{k}}^2}{\omega - E_{\mathbf{k}} + i\gamma_{\mathbf{k}}} + \frac{u_{\mathbf{k}}^2}{\omega + E_{\mathbf{k}} + i\gamma_{\mathbf{k}}} \end{pmatrix}. \quad (7)$$

This sort of behavior [Eq. (7)] can be derived on a microscopic level investigating the pairing interactions beyond the mean-field BCS framework.<sup>9</sup>

We moreover introduced in expression (7) some phenomenological damping rate  $\gamma_{\mathbf{k}}$ . For computational purposes, we use

$$\gamma_{\mathbf{k}} = \begin{cases} 0^+ & \text{for } T \leq T_c, \\ \gamma_{\mathbf{k}}(0) \frac{T - T_c}{T^* - T} & \text{for } T_c < T \leq T^* \end{cases} \quad (8)$$

and take its momentum variation  $\gamma_{\mathbf{k}} = \gamma^2 / (\gamma + \frac{|\xi_{\mathbf{k}S}|}{1000})$ , where parameter  $\gamma \equiv \gamma_{\mathbf{k}_F}$ . In Fig. 1, we illustrate the phenomenological temperature dependencies introduced in this section.

### III. UNCORRELATED QUANTUM DOT

To introduce the formalism of our calculations, we first start by analyzing the equilibrium case  $\mu_L = \mu_R$ . Using the Nambu notation, we can express the retarded Green's function of the QD through the Dyson equation

$$G_d^r(\omega)^{-1} = g_d^r(\omega)^{-1} - \Sigma_d^r(\omega), \quad (9)$$

with two contributions to the matrix self-energy  $\Sigma_d^r(\omega) = \Sigma_N^r(\omega) + \Sigma_S^r(\omega)$ . This problem can be solved exactly only for the case of noninteracting QD ( $U=0$ ) when

$$g_d^{0r}(\omega)^{-1} = \begin{pmatrix} \omega - \varepsilon_d + i0^+ & 0 \\ 0 & \omega + \varepsilon_d + i0^+ \end{pmatrix}, \quad (10)$$

and the corresponding self-energies simplify to<sup>10</sup>

$$\Sigma_N^{0r}(\omega) = \begin{pmatrix} \sum_{\mathbf{k}} \frac{|V_{\mathbf{k}N}|^2}{\omega - \xi_{\mathbf{k}N} + i0^+} & 0 \\ 0 & \sum_{\mathbf{k}} \frac{|V_{\mathbf{k}N}|^2}{\omega + \xi_{\mathbf{k}N} + i0^+} \end{pmatrix}, \quad (11)$$

$$\Sigma_S^{0r}(\omega) = \sum_{\mathbf{k}} |V_{\mathbf{k}S}|^2 \begin{pmatrix} \frac{u_{\mathbf{k}}^2}{\omega - E_{\mathbf{k}} + i\gamma_{\mathbf{k}}} + \frac{v_{\mathbf{k}}^2}{\omega + E_{\mathbf{k}} + i\gamma_{\mathbf{k}}} & \frac{u_{\mathbf{k}}v_{\mathbf{k}}}{\omega + E_{\mathbf{k}} + i\gamma_{\mathbf{k}}} - \frac{u_{\mathbf{k}}v_{\mathbf{k}}}{\omega - E_{\mathbf{k}} + i\gamma_{\mathbf{k}}} \\ \frac{u_{\mathbf{k}}v_{\mathbf{k}}}{\omega + E_{\mathbf{k}} + i\gamma_{\mathbf{k}}} - \frac{u_{\mathbf{k}}v_{\mathbf{k}}}{\omega - E_{\mathbf{k}} + i\gamma_{\mathbf{k}}} & \frac{v_{\mathbf{k}}^2}{\omega - E_{\mathbf{k}} + i\gamma_{\mathbf{k}}} + \frac{u_{\mathbf{k}}^2}{\omega + E_{\mathbf{k}} + i\gamma_{\mathbf{k}}} \end{pmatrix}. \quad (12)$$

Proper choice of the coefficient  $u_{\mathbf{k}}v_{\mathbf{k}} = \frac{\Delta_{\mathbf{k},sc}}{2E_{\mathbf{k}}}$  assures that the proximity effect appears in QD only for temperatures  $T < T_c$ . Above  $T_c$ , the pseudogap affects the QD spectrum only via the diagonal parts of Eq. (12).

The hybridization coupling  $V_{\mathbf{k}\beta}$  can be conveniently replaced by the weighted density function  $\Gamma_{\beta}(\omega) = 2\pi \sum_{\mathbf{k}} |V_{\mathbf{k}\beta}|^2 \delta(\omega - \varepsilon_{\mathbf{k}\beta})$ . For both electrodes being normal, the QD spectral function  $\rho_d(\omega) = -\frac{1}{\pi} G_{d11}^r(\omega)$  acquires a Lorentzian shape centered around the single particle level  $\varepsilon_d$  (see the dashed line in Fig. 2) with the effective broadening  $\Gamma = \Gamma_N + \Gamma_S$ .

If one electrode is superconducting with an isotropic ( $\mathbf{k}$  independent) energy gap, we notice several qualitative as well as quantitative differences of the QD spectrum.

(i) Since  $S$  electrons can occupy no states in the energy gap  $|\omega| < \Delta$ , thereby the line broadening gets reduced (by 50% when  $\Gamma_S = \Gamma_N$ ) and, in consequence, the QD peak around  $\varepsilon_d$  becomes narrower.

(ii) A large amount of  $S$  electron states is accumulated near  $\omega = \pm\Delta$  (i.e., at the square root divergences in the density of the  $S$  lead). Efficiency of the hybridization  $V_{\mathbf{k}S}$  is considerably enhanced, depleting the QD states at  $\omega = \pm\Delta$ .

(iii) A role of well defined quasiparticles in the superconducting state is played by the electron pairs. Due to the hybridization  $V_{\mathbf{k}S}$ , such particle-hole mixing is also transferred onto the QD spectrum (the proximity effect). In Fig. 2, we notice that besides the Lorentzian peak centered around  $\varepsilon_d$ , there also appears its tiny mirror reflection at  $-\varepsilon_d$ .

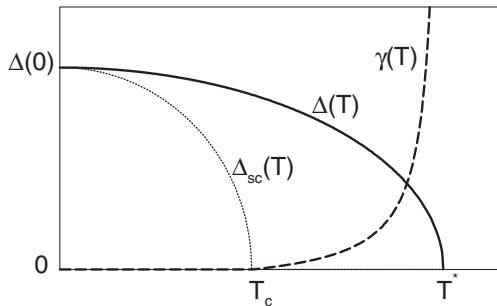


FIG. 1. Temperature dependence of the single particle gap  $\Delta(T)$  (solid line), the damping rate  $\gamma(T)$  (dashed line), and the superconducting order parameter  $\Delta_{sc}(T)$  (dotted line).

To provide the arguments for the above mentioned effects, we plot in Fig. 3 the diagonal and off-diagonal parts of the matrix self-energy  $\Sigma_d(\omega)$ . An odd symmetry of  $\text{Im}[\Sigma_{12}(\omega)]$  gives a nonvanishing  $\text{Re}[\Sigma_{12}(\omega)]$  for all energies located inside the energy gap  $|\omega| < \Delta$ . In diagonal term  $\Sigma_{11}(\omega)$ , the imaginary part is even (and negative) while the real part is odd (therefore vanishing at  $\omega=0$ ). Similar quantitative behavior of the matrix self-energy  $\Sigma_d(\omega)$  has been reported by several authors.<sup>11-14</sup> However, to our knowledge, no clear evidence of the particle-hole mixing (see Fig. 4) has been emphasized so far. We would like to stress that splitting of the Lorentzian inside the superconducting gap into the particle and hole peaks has nothing to do with the Kondo state; a sole proximity effect is responsible for it. After this paper was submitted, we noticed that the same results have been obtained by Tanaka *et al.*<sup>15</sup> using the numerical renormalization group calculations.

#### IV. STRONG CORRELATION LIMIT

It is known from the theoretical<sup>16</sup> and experimental studies<sup>17,18</sup> that the Coulomb interactions have a remarkable influence on transport properties through the QD. In particular, such correlations are responsible for the Coulomb blockade (observed by oscillations of the differential conductance)

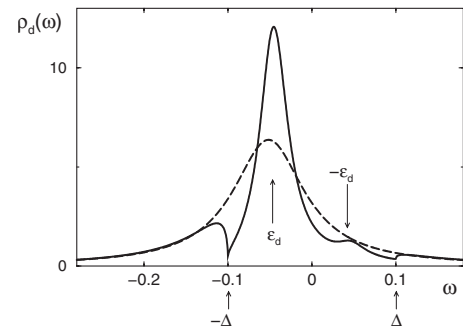


FIG. 2. Spectral function  $\rho_d(\omega)$  of the QD for  $U=0$  with the right hand side electrode being in a superconducting state (solid line) and in a normal state (dashed line). We used the isotropic energy gap  $\Delta_{\mathbf{k}}=0.1D$  and  $\varepsilon_d=-0.05D$ ,  $\Gamma_{\beta}=0.05D$ , and  $\gamma=0.01D$  and set the half bandwidth  $D$  as a unit for energies.

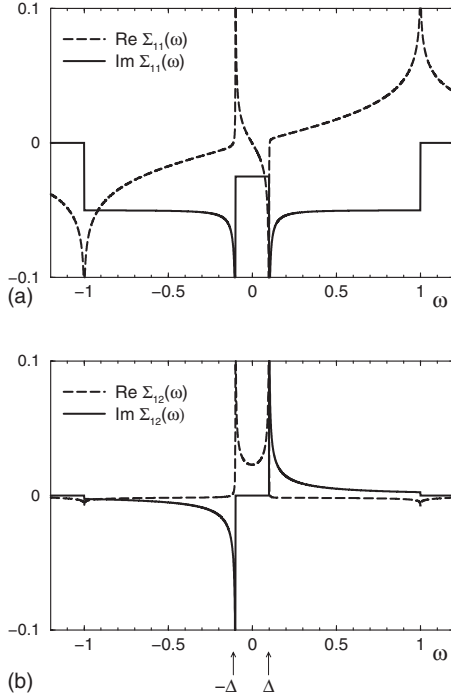


FIG. 3. The real and imaginary parts of the matrix self-energy for the diagonal  $\Sigma_{11}^r(\omega)$  (top panel) and off-diagonal  $\Sigma_{12}^r(\omega)$  (bottom panel) terms. We used the same set of parameters as in Fig. 1.

and, at sufficiently low temperatures, produce the Kondo resonance leading to enhancement of the conductance to the unitary limit value  $2e^2/h$ .

In this section, we consider the correlations focusing on the extreme limit of  $U=\infty$ . Under such condition, no double occupancy of the QD is allowed, and one expects it to have a tremendous effect on the charge tunneling, especially in the anomalous channels involving the electron pairs.

Excluding the doubly occupied states from the Hilbert space can be formally achieved using the auxiliary fields

$$\hat{d}_\sigma^\dagger = \hat{f}_\sigma^\dagger \hat{b}, \quad \hat{d}_\sigma = \hat{b}^\dagger \hat{f}_\sigma, \quad (13)$$

where the boson  $\hat{b}^{(\dagger)}$  and fermion operators  $\hat{f}_\sigma^{(\dagger)}$  correspond to an annihilation (creation) of the empty and singly occupied states on the QD. These new fields must obey the local constraint  $\hat{b}^\dagger \hat{b} + \sum_\sigma \hat{f}_\sigma^\dagger \hat{f}_\sigma = 1$ .

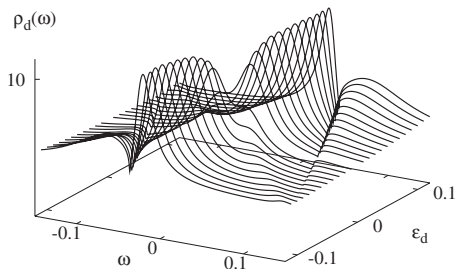


FIG. 4. The ground state spectral function  $\rho_d(\omega)$  of the QD for  $U=0$  versus varying position of the energy level  $\varepsilon_d$ . One can note a clear particle-hole mixing (two Lorentzians built around  $\pm\varepsilon_d$ ).

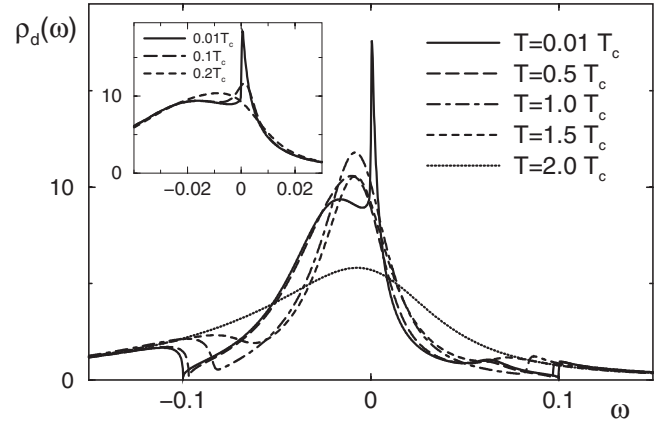


FIG. 5. Spectral function  $\rho_d(\omega)$  of the QD in the limit  $U=\infty$  obtained for  $\varepsilon_d=-0.05D$ ,  $\Gamma_\beta=0.01D$  assuming the isotropic energy gap  $\Delta_{\mathbf{k}}(T=0)=0.1D$  and  $T^* = 2T_c$ .

There are various methods to deal with the local constraint. For simplicity, we apply here the technique proposed by Le Guillou and Ragoucy,<sup>19</sup> where projecting out the doubly occupied states is achieved by appropriate commutation relations between the operators of auxiliary fields. For the present context [Eq. (1)], some necessary technical details have been previously discussed in Ref. 10.

In the limit  $U=\infty$ , the Dyson equation [Eq. (9)] can be solved using the renormalized propagator  $g_d^r(\omega) = (1 - n_{-\sigma})g_d^{r0}(\omega)$  and the matrix self-energy

$$\Sigma_\beta^r(\omega) = [\Sigma_\beta^{0r}(\omega) + \Sigma_\beta^{lr}(\omega)]/(1 - n_{-\sigma}), \quad (14)$$

where the contribution  $\Sigma_\beta^{0r}$  of noninteracting electrons is given in Eqs. (11) and (12). The other contribution  $\Sigma_\beta^{lr}$  originates from the correlations and, under appropriate conditions, leads to the Kondo effect.<sup>16</sup> One finds<sup>10</sup>

$$\Sigma_\beta^{lr}(\omega) = n_{\mathbf{k}\beta} \tau_3 \Sigma_\beta^{0r}(\omega) \tau_3, \quad (15)$$

where  $\tau_3$  is the Pauli matrix and  $n_{\mathbf{k}\beta}$  denotes an average occupancy of the  $\mathbf{k}$  momentum in the  $\beta$ th lead given by

$$n_{\mathbf{k}\beta} = \begin{cases} \left[ 1 + \exp\left(\frac{\xi_{\mathbf{k}N}}{k_B T}\right) \right]^{-1} & \text{for } \beta = N \\ \frac{1}{2} \left[ 1 - \frac{\xi_{\mathbf{k}S}}{E_{\mathbf{k}}} \tanh\left(\frac{E_{\mathbf{k}}}{2k_B T}\right) \right] & \text{for } \beta = S. \end{cases} \quad (16)$$

In Fig. 5, we show the spectral function  $\rho_d(\omega)$  calculated for several temperatures in both the superconducting and pseudogap states. In a comparison with the previous situation  $U=0$ , we can notice the following:

(i) For temperatures  $T < T_c$ , there are visible two Lorentzian peaks; however, their positions are a bit shifted from  $\pm\varepsilon_d$  because of a finite real part of the matrix self-energy (14).

(ii) For very low temperatures ( $T < T_K$ ), there appears a narrow Kondo resonance at the Fermi energy associated with the spin singlet made of the QD and itinerant electrons (see the inset of Fig. 5).

(iii) In the pseudogap regime above  $T_c$ , we no longer observe a tiny Lorentzian at  $\omega \approx -\varepsilon_d$  and simultaneously a dip of the spectral function at  $|\omega| = \pm \Delta_{pg}(T)$  gets smeared because of the damping effects.

For the particular set of parameters  $\Gamma_\beta = 0.01D$ ,  $\varepsilon_d = -0.05D$  used in Fig. 5, we estimate that the Kondo peak disappears for temperatures higher than  $T_K \approx 0.15T_c$ . For temperatures exceeding  $T^*$ , the QD spectrum evolves back to its single Lorentzian peak centered around  $\varepsilon_d$ .

## V. TRANSPORT PROPERTIES

In order to study the nonequilibrium physics, we use the Keldysh formalism. Applying a bias  $V$  leads to imbalance of the chemical potentials  $\mu_N - \mu_S = eV$ , which induces the charge current  $J(V) = -e \frac{d}{dt} \sum_{\mathbf{k}, \sigma} \langle c_{\mathbf{k}N\sigma}^\dagger c_{\mathbf{k}N\sigma} \rangle$  through the QD.

Following the procedure described previously,<sup>10</sup> we express the charge current  $J(V)$  in terms of the following contributions:

$$J = J_{11} + J_{12} + J_{22} + J_A. \quad (17)$$

The first three components in Eq. (17) have the Landauer-type structure

$$J_{ij}(V) = \frac{2e}{h} \int d\omega T_{ij}(V) [f(\omega - eV) - f(\omega)], \quad (18)$$

with the transmittances correspondingly defined by

$$T_{11}(V) = -\text{Im} \sum_{11,S}^r |G_{11}|^2 \Gamma_N(\omega), \quad (19)$$

$$T_{12}(V) = -2 \text{Im} \sum_{12,S}^r \text{Re}[G_{11} G_{12}^*] \Gamma_N(\omega), \quad (20)$$

$$T_{22}(V) = -\text{Im} \sum_{22,S}^r |G_{12}|^2 \Gamma_N(\omega). \quad (21)$$

The last contribution describes the Andreev current

$$J_A(V) = \frac{2e}{h} \int d\omega T_A(V) [f(\omega - eV) - f(\omega + eV)], \quad (22)$$

where

$$T_A(V) = -\text{Im} \sum_{22,N}^r |G_{12}|^2 \Gamma_N(\omega). \quad (23)$$

This type of current [Eq. (22)] arises when electron from the  $N$  lead is converted into the Cooper pair in the  $S$  electrode and simultaneously a hole is reflected back to the  $N$  lead. For a detailed discussion of such anomalous Andreev current, see, for instance, the recent review article.<sup>6</sup> In a case when the both leads are normal (i.e.,  $\Delta \rightarrow 0$ ), there survives only  $J_{11}(V)$  current and its transmittance (19) simplifies to the Meir-Weingreen form.<sup>16</sup>

In Fig. 6, we plot the differential conductance  $G(V, T) = dJ(V)/dV$  as a function of the external bias  $V$  for a set of representative temperatures. In the superconducting state, we clearly notice a strong suppression of the charge current at small voltages  $|eV| \leq \Delta(T)$ . Due to energy gap in the spectrum of  $S$  electrons, the tunneling occurs at small temperatures mainly through the Andreev channel. However, below  $T_c$ , the Andreev conductance  $G_A(V, T)$  is almost an order of

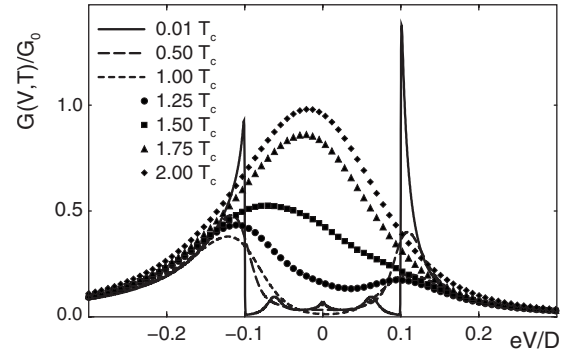


FIG. 6. The differential conductance  $G(V, T)$  versus the applied bias  $V$  for a representative set of temperatures in the superconducting region (lines) and for the pseudogap phase (symbols). We used the same set of parameters as in Fig. 5, and conductance is expressed in units of  $G_0 \equiv G(0, T^*)$ .

magnitude smaller than the normal state conductance  $G(V, T^*)$ .

For temperatures below  $T_K$ , there forms the Kondo peak (see Fig. 5) which has an indirect effect on the differential conductance at small biases  $|V|$ . From numerical calculations, we find that the Kondo peak enhances the zero-bias conductance (compare the panels of Fig. 8) through the Andreev scattering. This *zero-bias anomaly* is rather residual as compared to its efficiency for the N-QD-N junctions.<sup>16</sup> We checked that at temperatures below  $T_K$ , the zero-bias conductance  $G(0, T)$  fits very well the universal parabolic variation which is characteristic for the Kondo regime.

The limit  $\frac{T_K}{T_c} < 1$  has been previously addressed by other authors who used the mean-field theory for the auxiliary fields<sup>11</sup> and the non-crossing approximation (NCA) scheme supplemented by additional diagrams responsible for the anomalous channels of the transport.<sup>13</sup> The authors of Ref. 11 concluded that the zero-bias enhancement is partly suppressed for the N-QD-S junctions. In our present study, we do find an enhancement of the Andreev conductance due the Kondo resonance but actually this effect is so residual that it has been overlooked in the former studies of our group.<sup>10</sup> We hope that, nevertheless, this fragile effect could be somehow resolved experimentally.

For higher voltages, exceeding  $\Delta(T)$ , a dominant part of the charge transport comes from the normal current  $J_{11}(V)$ . In Fig. 7, we show each contribution to the total conductance at small temperature  $T < T_K < T_c$ . The anomalous channels  $J_{12}(V)$  and  $J_{22}(V)$  are activated slightly outside the energy gap and, like  $J_A(V)$ , they quickly diminish for an increasing bias  $|V|$ .

The in-gap conductance arising from the Andreev current is very sensitive to temperature (see Fig. 8). Already at  $T \sim T_K$ , the Kondo peak starts to be washed out and this leads to a concomitant disappearance of the zero-bias anomaly. Upon further increasing the temperature, there occurs a gradual suppression of the Andreev current which completely vanishes when  $T \rightarrow T_c^-$ .

For temperatures above  $T_c$ , the charge current is transmitted only via the normal  $J_{11}(V)$  channel. With increase of

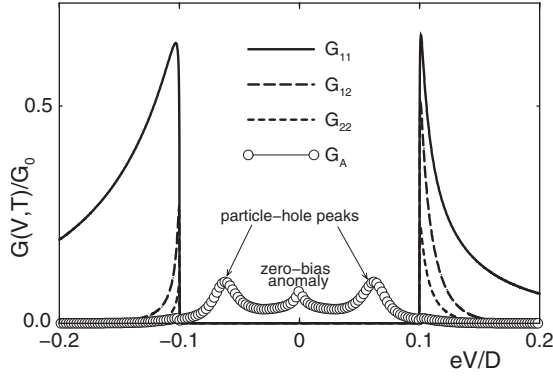


FIG. 7. Contributions of the normal channel  $G_{11}$  (solid line) and anomalous channels  $G_{12}$  (long-dashed line),  $G_{22}$  (short-dashed line), and  $G_A$  (circles) to the total differential conductance  $G(V, T)$  for temperature  $T=0.01T_c$  below  $T_K$ . All parameters have the same values as in Fig. 5.

temperature, the pseudogap is gradually filled in (see Fig. 6); therefore the zero-bias conductance smoothly increases, reaching a local maximum at  $T^*$ . In the normal state (which, in our case, corresponds to temperatures above  $T^*$ ), the differential conductance starts to fall off exponentially with respect to  $T$ . Let us remark that the differences in variation of the zero-bias differential conductances  $G(0, T)$  of superconductors with and without pseudogap shown in Fig. 9 could be a sensitive method for identifying the temperature region of the incoherent electron pairs.

## VI. *d*-WAVE SUPERCONDUCTOR

In high temperature superconductors (HTSCs), the electron (hole) pairs are formed locally, practically between the neighboring sites of  $\text{CuO}_2$  planes. The energy gap is anisotropic,  $\Delta_{\mathbf{k}} = \Delta(T) \cos 2\phi$ , where  $\phi$  stands for an azimuthal angle within the superconducting planes. In this section, we show that the fourfold symmetry of such anisotropic  $\Delta_{\mathbf{k}}$

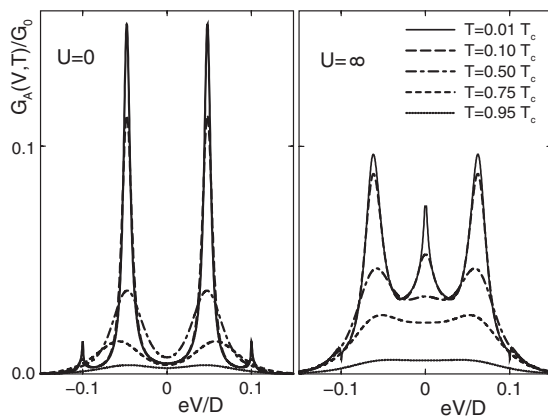


FIG. 8. The differential conductance  $G_A(V, T)$  of the Andreev current computed for a number of temperatures for  $U=0$  (left-side panel) and  $U=\infty$  (right-side panel). Notice the zero-bias enhancement (the middle peak) which is due to the Kondo resonance. Above  $T_c$ , the Andreev current vanishes (Ref. 6).

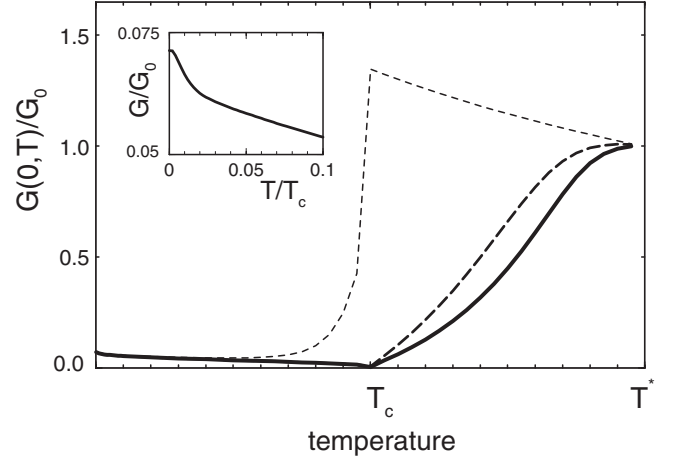


FIG. 9. Temperature dependence of the zero-bias differential conductance  $G(V=0, T)$  of the N-QD-S junction for the set of parameters used in Fig. 5. The thin dashed curve refers to the normal superconductor, while the thick lines describe the superconductor with a pseudogap, where the damping rate is  $\gamma=0.01D$  (solid curve) and  $\gamma=0.02D$  (dashed curve). Inset shows the enhancement at low temperatures due to the Kondo resonance.

strongly affects the characteristics of charge tunneling between the conducting STM tip, QD, and the superconducting electrode.

It is known on general grounds that impurities affect the *d*-wave (anisotropic) and *s*-wave (isotropic) superconductors in a qualitatively different way. According to the Anderson's theorem, paramagnetic impurities do not break the pairs in isotropic superconductors (unless the scattering is strong enough) while they have a detrimental influence on the *d*-wave superconductors.<sup>20</sup> In configuration of tunneling junctions (where QDs play analogous role to impurities), these properties can be expected to manifest, for instance, in the differential conductance (in much the same way as the Kondo effect shows up in the tunneling junctions and in the bulk materials). In what follows, we briefly consider two representative situations for tunneling (a) perpendicular and (b) parallel to the  $\text{CO}_2$  planes of high temperature superconductors.

### A. Perpendicular tunneling

If tunneling occurs along the  $z$  axis, we can consider the matrix elements  $V_{\mathbf{k}S}$  to be invariant under rotations of  $\phi$  by  $90^\circ$  within the  $\text{CuO}_2$  plane. From the symmetry reasons, the off-diagonal terms of the self-energies (12) and (14) cancel out after integration with respect to all orientations of two-dimensional  $\mathbf{k}$  vector. Thus, the *d*-wave superconducting energy gap  $\Delta_{\mathbf{k}}$  enters the QD Green's function  $G_d^r$  only through the diagonal part.

Assuming the constant matrix elements  $V_{\mathbf{k}S} \approx V_S$  for the physically relevant states (i.e., for momenta near the Fermi surface), we obtain the following imaginary part:

$$\text{Im} \Sigma_{S,11}^{0r}(\omega) = \text{Im} \Sigma_{S,22}^{0r}(-\omega) \equiv \Gamma_S(\omega), \quad (24)$$

where  $\Gamma_S(\omega)$  is a weighted density of states of the *d*-wave superconducting electrode,

$$\Gamma_S(\omega) = |V_S|^2 \text{Re} \left\langle \frac{\omega + i\gamma}{\sqrt{[\omega + i\gamma]^2 - \Delta^2(T) \cos^2(2\phi)}} \right\rangle_\phi, \quad (25)$$

and  $\langle \dots \rangle_\phi$  denotes averaging over the angle  $\phi$ . The same structure of effective coupling [Eq. (25)] has also been recently inferred from the STM studies<sup>21</sup> when exploring the HTSC materials in temperature region below and above  $T_c$ . Authors figured out that the lifetime broadening  $\gamma$  is very small at low temperatures and can be fitted by a finite value for higher temperatures (in the pseudogap regime). The effective coupling  $\Gamma_S(\omega)$  has a characteristic V-shape energy dependence, which, above  $T_c$ , gets broadened at  $\omega \sim \pm\Delta(T)$  due to the damping effects as shown in the top panel of Fig. 10.

Total self-energy (14) of the strongly correlated QD consists of  $\Sigma_S^{0r}$ , and another term given by Eq. (15). Both terms affect the retarded Green's function  $G_d^r(\omega)$ , and the resulting QD spectrum  $\rho_d(\omega)$  is shown in the middle panel of Fig. 10. In particular, we notice that (a) for  $T < T_K$  (assumed here to be smaller than  $T_c$ ), there is again a formation of the Kondo resonance; (b) for  $T_K < T < T_c$ , the Kondo resonance is gone while still the sharp energy gap features exist at  $\omega = \pm\Delta(T)$ ; and (c) in the pseudogap region  $T_c < T < T^*$ , the damping  $\gamma \neq 0$  gradually smears out the gap features.

For tunneling perpendicular to  $\text{CuO}_2$  planes (as nicely illustrated in Fig. 1 of Ref. 22), the diagonal structure of the matrix Green's function [Eq. (9)] signals an absence of the proximity effect (recall the pair-breaking influence of impurities on  $d$ -wave superconductors). Under such conditions, the charge current [Eq. (17)] flows through the normal channel whose transmittance (19) simplifies to the well known formula<sup>16</sup>

$$T_{11}(\omega) = \frac{\Gamma_S(\omega)\Gamma_N}{\Gamma_S(\omega) + \Gamma_N} \rho(\omega). \quad (26)$$

This quantity [Eq. (26)] determines the differential conductance. At low temperatures and in the limit  $|V| \rightarrow 0$ , the conductance is suppressed (see the bottom panel of Fig. 10) due to  $\Gamma_S(\omega)$ . Disappearance of the zero-bias conductance at low temperatures makes it hence insensitive to the Kondo effect and this property is qualitatively different in comparison with the behavior discussed in previous sections for the isotropic superconductor.

### B. Parallel tunneling

For tunneling parallel to the superconducting  $\text{CuO}_2$  planes, a rotational symmetry of the model [Eq. (1)] breaks down. In general, it is then a complicated issue to properly treat the geometry of an interface. In principle, one should construct and numerically solve a corresponding set of the Bogoliubov–de Gennes equations,<sup>23</sup> but such strategy is beyond a scope of the present study. To get some insight of the underlying physics, we proceed in assuming that momentum is conserved in the plane of the interface.<sup>24</sup> To dismiss the rotational symmetry, we propose factorizing  $V_{\mathbf{k}S}$  as function

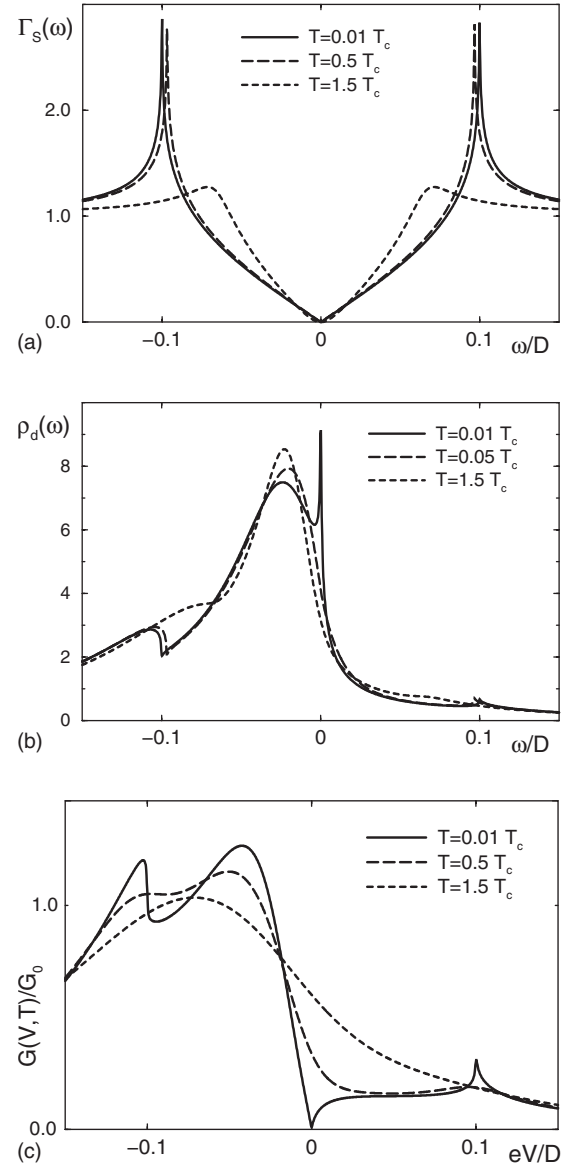


FIG. 10. Effective coupling  $\Gamma_S(\omega)$  (top panel), spectral function  $\rho_d(\omega)$  (middle panel), and bias  $V$  dependence of the differential conductance  $G(V, T)$  for a perpendicular tunneling to the  $d$ -wave superconductor. We used the correlated quantum dot ( $U = \infty$ ) with the energy level  $\varepsilon_d = -0.08D$  and considered three representative temperatures:  $T < T_K < T_c$  (solid lines),  $T_K < T < T_c$  (long-dashed lines), and  $T_c < T < T^*$  (short-dashed lines).

of  $\mathbf{k}$ -vector directions promoting the tunneling predominantly along  $x$  axis,

$$|V_{\mathbf{k}S}| = |V_S|^2 \mathcal{N}[\alpha] e^{-\alpha\phi^2}, \quad (27)$$

where  $\phi \in [-\pi, \pi]$  and  $\mathcal{N}[\alpha]$  is a normalizing factor. Instead of Eq. (27), other types of parametrizations can be used, but we believe that one would nevertheless obtain the same conclusions.

Replacing  $\mathbf{k}$  summation by  $\sum_{\mathbf{k}} = \int_{-D}^D \frac{d\xi_S}{2D} \int_{-\pi/2}^{\pi/2} \frac{d\phi}{2\pi}$ , we can determine the matrix self-energy (12),

$$\Sigma_S^{0r}(\omega) = |V_S|^2 \mathcal{N}[\alpha] \int_{-D}^D \frac{d\xi_S}{2D} \int_{-\pi}^{\pi} \frac{d\phi}{2\pi} e^{-\alpha\phi^2} \begin{pmatrix} \frac{\omega + i\gamma + \xi_S}{(\omega + i\gamma)^2 - \xi_S^2 - \Delta^2(T)\cos^2(2\phi)} & \frac{-\Delta(T)\cos(2\phi)}{(\omega + i\gamma)^2 - \xi_S^2 - \Delta^2(T)\cos^2(2\phi)} \\ -\Delta(T)\cos 2\phi & \frac{\omega + i\gamma - \xi_S}{(\omega + i\gamma)^2 - \xi_S^2 - \Delta^2(T)\cos^2(2\phi)} \end{pmatrix} \quad (28)$$

and also the correlation contribution  $\Sigma_i(\omega)$  defined in Eq. (15). For sufficiently large asymmetries (controlled here by the parameter  $\alpha$ ), we almost reproduce the behavior of the isotropic superconductor. For instance, in Fig. 11, we plot the differential conductance of the Andreev current for  $\alpha=1$ . Again, we notice the appearance the zero-bias anomaly below  $T_K$  together with a systematic decrease of the in-gap conductance toward  $T \rightarrow T_c$  (compare it to the right hand side panel of Fig. 8).

Practically, by varying  $\alpha$ , we can interpolate between the limits of the tunneling perpendicular to the  $d$ -wave superconductor presented in Sec. VI A. (when  $\alpha=0$ ) and tunneling to the isotropic superconductor discussed in Sec. V (when  $\alpha \rightarrow \infty$ ). While formally it is rather obvious, we support this conclusion showing in Fig. 12 the zero-bias conductance starting from the region of small values  $\alpha$ .

## VII. CONCLUSIONS

We have investigated a charge tunneling through the quantum dot located between the normal and superconducting leads. So far, such situation has been addressed by several authors<sup>10-14,25</sup> using various methods to account for the correlations, and it has been shown that the QD (coupled to isotropic superconductor) absorbs the off-diagonal order. Here, we emphasize that this proximity effect is further responsible for splitting the QD spectrum into the particle and hole peaks whenever  $|\varepsilon_d| \leq \Delta$ . Independently, the same conclusion has been recently reached by Tanaka *et al.*<sup>15</sup> from the renormalization group studies. In practice, such a phenom-

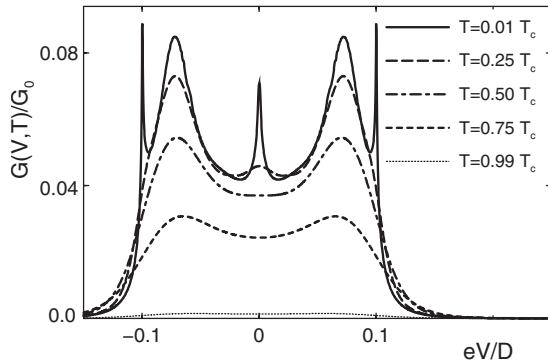


FIG. 11. Differential conductance of the Andreev current for the tunneling along the  $x$  axis of the  $d$ -wave superconductor. For computations, we used  $\Delta(0)=0.1D$ ,  $\alpha=1$  and considered the strongly correlated quantum dot ( $U=\infty$ ) with the same set of parameters as in Fig. 8.

enon might be observed measuring the differential conductance upon varying the gate voltage across N-QD-S junction.

Due to the on-dot correlations  $U$ , at sufficiently low temperatures, the Kondo state can appear.<sup>16</sup> In tunneling junctions containing isotropic superconductors (where the low energy excitations are “frozen” because of the Cooper pair binding), the Kondo effect arises owing to the normal lead electrons and it has an influence on the transport properties. At low temperatures, the normal channel  $J_{11}(V)$  is forbidden for  $|eV| < \Delta$ ; therefore, charge can be transferred solely through the Andreev channel. Although the magnitude of the Andreev current is small,<sup>6</sup> nevertheless, in analogy to the zero-bias Kondo anomaly of N-QD-N junctions,<sup>16,17</sup> we do find a similar (though tiny) enhancement for the N-QD-S setup.

We extended our study also on the superconductors which exhibit the pseudogap above  $T_c$ . We have found that temperature dependence of the zero-bias conductance  $G(0,T)$  is completely different compared to the conventional superconductors. In the latter case,  $G(0,T)$  rises abruptly to its normal state value when passing  $T_c$  (see the thin dashed curve in Fig. 9), while in the former, it has a nonmonotonous temperature variation with a marked minimum at  $T_c$  (the thick solid and dashed curves in Fig. 9). From a physical point of view, we can distinguish between the following three regimes: (a) for  $T < T_K$ , we note the enhancement of the zero-bias conductance; (b) in the range  $T_K < T < T_c$ , there is a systematic decrease of the Andreev current for  $T \rightarrow T_c$ , while still no other channel of the transport is allowed because of the finite gap; and (c) for  $T > T_c$ , the anomalous channels disappear and there is a continuous revival of the normal current through filling in the pseudogap. We believe that this unique temperature behavior could serve as a sensitive tool for probing the region  $T_c < T < T^*$  of the incoherent electron pairs.

There are some additional effects which might eventually play a role in practical realizations of the N-QD-S junctions.

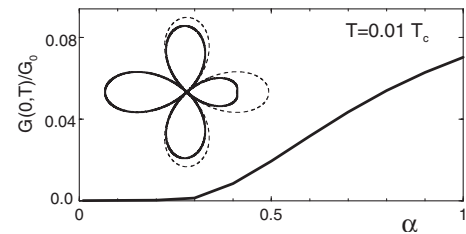


FIG. 12. The zero-bias value of the Andreev conductance  $G_A(0,T)$  as a function of the asymmetry parameter  $\alpha$  using the same model parameters as in Fig. 11 for  $T=0.1T_c$ . Inset shows the gap fraction  $\Delta_{\mathbf{k}}$  weighted by the angular factor  $e^{-\alpha\phi^2}$  for  $\alpha=0.1$  (thick solid line) and  $\alpha=0$  (thin dashed line).

One of them is the gap anisotropy, which, in HTSC materials, has the  $d$ -wave symmetry. This kind of a problem has been partly addressed in Ref. 22, where authors explored the charge current from a conducting STM tip to quasi-two-dimensional superconducting  $\text{CuO}_2$  planes via the apical oxygen atom (to be regarded as QD). Their study has been focused on the influence of inelastic scattering driven by the oxygen atoms' vibrations.

Here, we analyzed the effective charge currents for such  $d$ -wave function  $\Delta_{\mathbf{k}}$  considering two representative orientations of the STM tip with respect to the superconducting  $\text{CuO}_2$  planes. From various theoretical considerations, it is known that the Kondo state can show up in the gapless ( $d$ - or  $p$ -wave) superconductors.<sup>26,27</sup> The tip orientation has, how-

ever, a strong impact on the properties of N-QD-S tunneling junctions. We discussed this issue in some detail for the limit  $T_K \ll \Delta$  when the in-gap states qualitatively affect the low energy nonequilibrium transport. Our results can be regarded as complementary to analogous study of the QD attached to  $p$ -wave superconductor<sup>25</sup> for the other limit,  $T_K \gg \Delta$ , where the Kondo effect strongly dominates over the superconducting correlations.

#### ACKNOWLEDGMENTS

This work is partially supported by the Polish Committee of Scientific Research under Grant No. 2P03B06225. We thank M. Krawiec for valuable discussions.

- 
- <sup>1</sup>D. N. Basov and T. Timusk, *Rev. Mod. Phys.* **77**, 721 (2005); T. Timusk and B. Statt, *Rep. Prog. Phys.* **62**, 61 (1999).
- <sup>2</sup>Y. Wang, L. Li, M. J. Naughton, G. D. Gu, S. Uchida, and N. P. Ong, *Phys. Rev. Lett.* **95**, 247002 (2005).
- <sup>3</sup>J. Corson, L. Mallozzi, J. Orenstein, J. Eckstein, and I. Bozovic, *Nature (London)* **398**, 221 (1999).
- <sup>4</sup>O. Fisher, M. Kugler, I. Maggio-Aprile, Ch. Berthod, and Ch. Renner, *Rev. Mod. Phys.* **79**, 353 (2007).
- <sup>5</sup>A. Damascelli, Z. Hussain, and Z.-X. Shen, *Rev. Mod. Phys.* **75**, 473 (2003).
- <sup>6</sup>G. Deutscher, *Rev. Mod. Phys.* **77**, 109 (2005).
- <sup>7</sup>K. McElroy, J. Lee, J. A. Slezak, D.-H. Lee, H. Eisaki, S. Uchida, and J. C. Davis, *Science* **309**, 1048 (2005).
- <sup>8</sup>Q. Chin, J. Stajic, S. Tan, and K. Levin, *Phys. Rep.* **412**, 1 (2005).
- <sup>9</sup>J. M. Singer, M. H. Pedersen, T. Schneider, H. Beck, and H.-G. Matuttis, *Phys. Rev. B* **54**, 1286 (1996); Y. M. Vilc and A.-M. S. Tremblay, *J. Phys. I* **7**, 1309 (1997); T. Domański and J. Ranninger, *Phys. Rev. Lett.* **91**, 255301 (2003).
- <sup>10</sup>M. Krawiec and K. I. Wysokiński, *Supercond. Sci. Technol.* **17**, 103 (2004).
- <sup>11</sup>R. Fazio and R. Raimondi, *Phys. Rev. Lett.* **80**, 2913 (1998); **82**, 4950 (1998); P. Schwab and R. Raimondi, *Phys. Rev. B* **59**, 1637 (1999).
- <sup>12</sup>Q.-F. Sun, J. Wang, and T.-H. Lin, *Phys. Rev. B* **59**, 3831 (1999); Q.-F. Sun, H. Guo, and T.-H. Lin, *Phys. Rev. Lett.* **87**, 176601 (2001).
- <sup>13</sup>A. A. Clerk, V. Ambegaokar, and S. Hershfield, *Phys. Rev. B* **61**, 3555 (2000); A. A. Clerk and V. Ambegaokar, *ibid.* **61**, 9109 (2000).
- <sup>14</sup>J. C. Cuevas, A. L. Yeyati, and A. Martin-Rodero, *Phys. Rev. B* **63**, 094515 (2001).
- <sup>15</sup>Y. Tanaka, N. Kawakami, and A. Oguri, *J. Phys. Soc. Jpn.* **76**, 074701 (2007).
- <sup>16</sup>Y. Meir and N. S. Wingreen, *Phys. Rev. Lett.* **68**, 2512 (1992); Y. Meir, N. S. Wingreen, and P. A. Lee, *ibid.* **70**, 2601 (1993).
- <sup>17</sup>D. Goldhaber-Gordon, H. Shtrikman, D. Mahalu, D. Abusch-Magder, U. Mairav, and M. A. Kastner, *Nature (London)* **391**, 156 (1998).
- <sup>18</sup>S. De Franceschi, R. Hanson, W. G. van der Wiel, J. M. Elzerman, J. J. Wijkema, T. Fujisawa, S. Tarucha, and L. P. Kouwenhoven, *Phys. Rev. Lett.* **89**, 156801 (2002).
- <sup>19</sup>J. C. Le Guillou and E. Ragoucy, *Phys. Rev. B* **52**, 2403 (1995).
- <sup>20</sup>A. V. Balatsky, I. Vekhter, and J.-X. Zhu, *Rev. Mod. Phys.* **78**, 373 (2006).
- <sup>21</sup>K. K. Gomes, A. N. Pasupathy, A. Pushp, S. Ono, Y. Ando, and A. Yazdani, *Nature (London)* **447**, 569 (2007).
- <sup>22</sup>S. Pilgram, T. M. Rice, and M. Sigrist, *Phys. Rev. Lett.* **97**, 117003 (2006).
- <sup>23</sup>N. Stefanakis, *Phys. Rev. B* **66**, 024514 (2002).
- <sup>24</sup>Y. Tanaka, Yu. V. Nazarov, A. A. Golubov, and S. Kashiwaya, *Phys. Rev. B* **69**, 144519 (2004).
- <sup>25</sup>T. Aono, A. Golub, and Y. Avishai, *Phys. Rev. B* **68**, 045312 (2003); Y. Avishai, A. Golub, and A. D. Zaikin, *ibid.* **63**, 134515 (2001).
- <sup>26</sup>L. S. Borkowski and P. J. Hirschfeld, *Phys. Rev. B* **46**, 9274 (1992).
- <sup>27</sup>M. Vojta and R. Bulla, *Phys. Rev. B* **65**, 014511 (2001); M. Vojta, R. Zitler, R. Bulla, and Th. Pruschke, *ibid.* **66**, 134527 (2002); A. Polkovnikov, S. Sachdev, and M. Vojta, *Phys. Rev. Lett.* **86**, 296 (2001).